Physica C 167 (1990) 423–432
North-Holland

PREPARATION OF YBaCuO THIN FILMS ON VARIOUS SUBSTRATES BY LASER ABLATION

Influence of the substrate temperature

D.H.A. BLANK, D.J. ADELERHOF, J. FLOKSTRA and H. ROGALLA
Faculty of Applied Physics, University of Twente, P.O.B. 217, 7500 AE Enschede, The Netherlands

Received 5 February 1990
Revised manuscript received 12 March 1990

High-quality $YBa_2Cu_3O_{7-\delta}$ films were prepared in situ by laser ablation on $SrTiO_3$ (100), on MgO (100) and on Si (111) + ZrO_2 buffer layer. We especially investigated the influence of the substrate temperature. In similar preparation circumstances zero resistivity has been achieved for films on $SrTiO_3$ up to 89.5 K, on MgO up to 84.6 K and on Si(+ZrO_2) up to 83.5 K. X-ray diffraction analysis was used to study the growth conditions of the films, and to determine the oxygen stoichiometry. The films deposited at substrate temperatures above 720°C show pure *c*-axis orientation with an oxygen deficiency $\delta < 0.1$. Interdiffusion between substrate and layer, analyzed with Auger sputter profiling, could not be observed. The grains of the films on Si + ZrO_2, studied by scanning electron microscopy, are caused by the polycrystalline buffer layer. These grains largely determine the physical properties of the deposited layer.

Critical current measurements were carried out using wet chemically etched microbridges on the different substrates. At $T = 77$ K the values are in the range from 3×10^6 A/cm^2 for films on $SrTiO_3$ to 2×10^3 A/cm^2 in the case of Si + ZrO_2. The extrapolated resistivity at $T = 0$ is found to be proportional to the temperature width of the superconducting transition.

1. Introduction

High-quality high-T_c superconducting films have been fabricated by many different techniques [1–3]. Especially due to the development of in situ preparation of YBaCuO films it is possible to produce thin films with good physical properties such as perfect *c*-axis orientation, large critical current densities, and smooth surfaces [4–6]. The relatively low deposition temperature is an important feature of the in situ process.

Laser ablation has some distinct advantages in comparison with other deposition techniques. The experimental equipment is relatively simple. The substrate temperature can be varied without disturbing the ablation process. There is a free choice of gas, in our case oxygen, and pressure in the ablation chamber. This enables the adjustment of the oxygen concentration of the high-T_c material. A further advantage of the laser ablation technique is the high deposition rate. The effect of the interdiffusion between substrate and deposited layer can be minimized by choosing the highest deposition rate without disturbing the growth kinetics of the film.

The broad interest in the deposition of YBaCuO on silicon stems from the possible integration of high-T_c superconductors with semiconductors for microelectronic applications. ZrO_2 is shown to be a promising buffer layer with the use of Si [7]. Venkatesan et al. [8] showed the positive effect of the relative low deposition temperature on the interdiffusion, using the in situ preparation method.

In this layer we present a parameter study on the fabrication of $YBa_2Cu_3O_{7-\delta}$ films by means of laser ablation on Si (111) + a 250 nm thick ZrO_2 buffer layer, and compare the results with the data from a similar study for $SrTiO_3$ (100) and MgO (100) substrates. In particular, the influence of the substrate temperature was investigated. At low deposition temperatures one expects a disturbance of the growth of the YBaCuO layer leading to reduced oxygen concentration and a less pronounced *c*-axis orientation. At high deposition temperatures interdiffusion between layer and substrate may occur and, because of

the enhanced mobility at the grain boundaries, the occurrence of grains becomes important. The effects of the deposition at too low and too high substrate temperatures can be clearly seen from temperature-dependent resistivity measurements.

To investigate crystallographic orientations of the films and to determine the oxygen stoichiometry in relation to the dimensions of the unit cell, X-ray diffraction measurements were performed.

Interdiffusion between the silicon substrate and YBaCuO prepared at different deposition temperatures was studied using Auger Electron Spectroscopy (AES).

The microstructure of the surface of the thin films was determined using Scanning Electron Microscopy (SEM). Some attention was paid to the "particle problem", which can be a disadvantage of the laser ablation process.

2. Experimental details

The films were deposited with an excimer laser (Lambda Physic LPX 110 CC) in the XeCl operation mode (308 nm). The maximum laser pulse energy is about 150 mJ and the maximum pulse frequency is 100 Hz. An unstable resonator is used in order to obtain better focusing of the laser beam.

The ablation chamber, with an inner diameter of 40 cm, and a height of 20 cm, is turbo pumped and contains a rotatable target table, quarts windows for the laser beam and observation of the plasma a gas inlet, and a movable substrate holder. The substrate holder consists of a stainless steel plate heated by a NiCr (Thermo coax) wire and it can reach a temperature of up to 950 °C. The temperature of the substrate is measured with a pyrometer in combination with a thermocouple mounted inside a dummy substrate.

The target is a pellet of $YBa_2Cu_3O_{7-\delta}$ prepared by the citrate/pyrolysis method [9] and has a diameter of 16 mm. The spot size of the laser beam is typically 2 mm^2. In order to obtain the correct stoichiometry of the YBaCuO films, the substrate has to be placed at the outer edge of the plasma. The spatial extension and the shape of the plasma is influenced by the energy density of the laser beam, the density of the target, the oxygen pressure in the chamber and, to a lesser extent, by the laser pulse frequency. In our experiments we keep the energy density at about 2 J/cm^2. The oxygen pressure is 30 Pa and the pulse frequency in general is 2 Hz. The target to substrate distance is 25 to 35 mm. With these adjustments the deposition rate is typically 0.5 Å/shot. In our case the deposition time was about 30 min, for a film thickness between 250 and 300 nm.

To stabilize the substrate temperature and to clean the substrate, the ablation procedure consists of a preheating of the substrate at 770 °C for 30 min, followed by an adjustment of the above mentioned ablation parameters: pulse frequency, energy density and oxygen pressure. After deposition the film, with typical dimensions of 10×5 mm^2, is cooled down to room temperature in 1.5 h in an oxygen atmosphere of ambient pressure. No further annealing procedure is necessary to obtain good superconducting properties.

The DC resistivity measurements were carried out using a standard four-probe method with pressure contacts of gold. The current densities used in these measurements were between 1 and 10 A/cm^2. Microbridges of 10 μm wide and 100 μm long were structured in the films by wet chemical etching using standard photo resist and diluted H_3PO_4 (1:150) as the etchant. Such bridges were used for the critical current measurements.

X-ray diffraction patterns have been obtained by a Debye–Scherrer diffractometer with a Cu Kα source, SEM pictures were taken with a Philips PSEM 500 and Auger sputter profiles were made with a Perkin–Elmer PHI-600 Multiprobe.

3. Results

The substrate temperature during deposition is a crucial parameter, as is well known from the literature. The temperature of the substrate differs from that of the heater depending on the heat balance for the substrate. In this respect, the thermal contact resistance, which depends on the force at which the substrate is clamped onto the heater, is of importance. Also the thermal conductivity of the substrate and the emissivity have to be considered. The latter quantity can even change during the deposition of the YBaCuO layer. Finally, the plasma itself influ-

ences the surface temperature of the substrate. We found that the temperature of the substrate can be 150°C lower than that of the heater. For a comparison of the results obtained with the different substrates it is important to know the correct substrate temperature. Therefore the temperature is measured in two different ways. A thermocouple, which is placed in a dummy substrate, is used and the obtained data is verified with a pyrometer. In this way the correct value of the temperature can be given to within 15 K.

Resistivity measurements of YBaCuO films on the three substrate types, prepared at different substrate temperatures (T_{sub}), show similar temperature behaviour. All curves exhibit a linear temperature dependence of the resistivity above $T \approx 110$ K. The onset temperature, T_{ons}, varies from 88 to 91 K and is almost independent of T_{sub}. The temperature at which zero resistivity is reached (T_{zero}), however, is strongly dependent on T_{sub} and the substrate type. Table I gives an overview of the data obtained from the YBaCuO films on $SrTiO_3$, on MgO and on $Si+ZrO_2$.

In fig. 1, T_{zero} is given as a function of the substrate temperature for the three different substrates. We define this T_{zero} as the temperature at which the resistivity is less than 10^{-8} Ωcm. All films were prepared under the same ablation conditions, so that the results can be mutually compared. It is seen from the figure that in the case of $SrTiO_3$ good results ($T_{zero} > 88$ K) are obtained for $T_{sub} > 720$°C. The maximum value of T_{zero} for MgO is lower (85 K) and a broad optimum has been found in the temperature range from 730°C to 760°C. This optimum is more pronounced for the $Si+ZrO_2$ substrates. At higher values of T_{sub} the superconducting properties deteriorate. The highest reachable T_{zero} with these ablation parameters is 84 K.

The crystallographic properties of the deposited layers were studied by X-ray diffraction experiments. The data show perfectly *c*-axis oriented films. The intensities of the (00*l*) reflections of YBaCuO are of the same order of magnitude in the cases of $Si+ZrO_2$ and $SrTiO_3$, whereas the reflections for MgO are of considerably lower intensity. Figure 2 shows the intensities of the (005) reflections of the YBaCuO films on the three different substrates at various T_{sub}. The same figure depicts the (110/103) reflections. It is remarkable that these intensities are very small even at low deposition temperatures.

The oxygen content of the YBaCuO films is an important parameter for the superconducting properties. Because the films are made in situ, one expects a direct influence of the deposition temperature on the oxygen stoichiometry: the *a*-axis and *c*-axis increase, whereas the *b*-axis decreases with decreasing oxygen concentration. This behaviour was described by Cava et al. [10] and from their data we calculated the oxygen concentration from the 2θ values of the X-ray pattern. The results are given in fig. 3. The films made at high substrate temperatures have the highest oxygen content.

Special attention was paid to the interdiffusion between silicon, ZrO_2 and YBaCuO. For this purpose, depth profiles and line scans were carried out with AES. On the silicon (111) substrates an amorphous buffer layer of zirconium oxide was deposited by a sputter process. The buffer layer was crystallized at a temperature of 700°C for 30 min, just before the ablation process started. In fig. 4 the Auger sputter profile is given in the case of an YBaCuO film on $Si+ZrO_2$, deposited at 700°. The sputter rate was calibrated on 100 nm Ta_2O_5, as 46 nm/min. A clear separation between the YBaCuO, ZrO_2, and Si layers can be seen. With this depth profile also the homogeneity of the layer (e.g. the amount of elements Y, Ba, Cu and O during the deposition) becomes visible. No silicon has been found in the YBaCuO layer from these depth profiles. In the Auger sputter profile measurements, the detection limit for Si was 1%. With Auger line profiling parallel to the substrate, some indications of Si diffusion along the grain boundaries in the ZrO_2 buffer layer were found. The intensities of the peak to peak value of Si_2, corrected for topographic errors, are given in fig. 5 for a film deposited at a T_{sub} of 750°C. The SEM picture of the cleaved surface shows the granular structure of the ZrO_2 buffer layer and, although very small, an increase of the Si_2 intensity can be seen at the grain boundaries.

The sizes of the grains in the YBaCuO layer and in the polycrystalline ZrO_2 buffer layer on the Si substrate have been investigated by SEM. Figure 6 shows a picture of a YBaCuO bridge used for critical current measurements. It can be clearly seen that the film consists of grains with typical dimensions of 1 μm.

Table I
Some characteristic data of a number of YBaCuO films, with a typical thickness of 250 nm deposited on (100) $SrTiO_3$, (100) MgO and (111) Si + buffer layer of 250 nm ZrO_2. The films are prepared at different substrate temperatures T_{sub}. The resistivity at $T = 300$ K, 100 K and the extrapolated resistivity at $T = 0$ K are given. The table contains the onset and zero temperatures (T_{ons} and T_{zero}), using a measuring current density of 10 A/cm^2. For some films the critical current densities (I_{cc}) at $T = 77$ K are given, using microbridges with dimensions of 10 μm × 100 μm, and structured by wet-chemical etching.

ρ_{300} (μΩcm)	ρ_{100} (μΩcm)	ρ_{EX} (μΩcm)	T_{sub} (°C)	T_{ons} (K)	T_{zero} (K)	I_{cc} (A/cm^2)
$SrTiO_3$						
2295	2118	2030	600			
1086	603	361	610			
381	150	35	690	89	78	
195	75	15	730	90	87	5×10^5
150	54	6	750	91	89	2×10^6
126	45	4	775	90	89.5	3×10^6
MgO						
681	609	573	650	88	50	
405	321	279	660	82	62	
408	330	291	670	87	69	
405	225	135	685	88	75	
216	85	20.3	730	88	83.5	
188	75	18.4	740	88.5	83	
252	96	18	750	88	85	2×10^5
178	75	23.6	775	88.5	84.5	1×10^5
Si + ZrO_2						
4600	4600	4600	645	85	51	
2580	2260	2100	677	88	60	
566	326	206	700	90	79.6	
424	216	112	715	90	83.5	3×10^4 [a]
486	282	180	725	90	81.5	2×10^3
670	382	238	735	91	80.5	1×10^3
836	516	356	750	91	78.5	
6240	3160	1620	775	90	69	
6120	3520	2220	780	90	68	

[a] Measured for a film structured by laser ablation.

The polycrystalline buffer layer imposes this grain structure on the YBaCuO layer. This effect can be clearly demonstrated by chemical etching, because the grain boundaries are especially sensitive to the etching.

A disadvantage of laser ablation can be seen from fig. 6. Together with the (partially ionized) elements some droplets leave the target. They are responsible for the ball shaped particles on the film surface with a typical diameter of 1 μm. Although the film itself is very smooth, these particles make the surface rough and therefore not very suitable for multilayer applications. With optimization of the target with respect to density and grain size, we were able to decrease the number of particles, but further investigations have to be done to overcome this nuisance.

Critical current measurements were performed with the type of microbridges shown in fig. 6. In table I an overview is given of the results for the different substrates. The critical current in the case of the Si substrates is rather low. Resistivity measurements show a degradation of the film: the transition width becomes broader, due to the wet etching, whereas the films on $SrTiO_3$ were not deteriorated after the etching. Films on Si + ZrO_2 were also structured by the excimer laser, using a contact mask. In this case there is no influence on the transition width and the critical current in these films is one order of

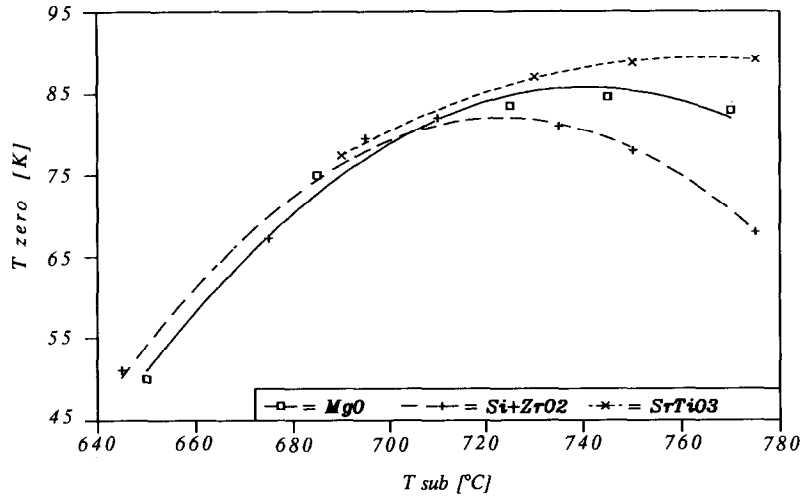

Fig. 1. T_{zero} as a function of the substrate temperature for three different substrates: $SrTiO_3$, MgO and $Si+ZrO_2$.

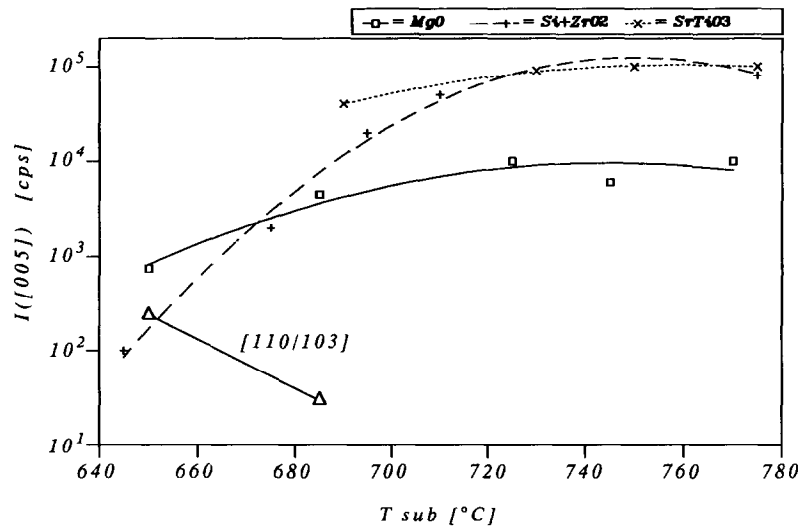

Fig. 2. The intensities of the (005) reflections of YBaCuO films on three different substrates at various T_{sub}. The triangles represent the (110/103) reflections of the YBaCuO films on MgO.

magnitude larger than the critical currents of the films structured by wet etching.

4. Discussion

Resistivity measurements contain a variety of valuable information about the electrical properties of thin films. Table I shows the obtained data from such measurements for a number of deposited films. For our measurements it turned out that the value of the resistivity at room temperature ($\rho_{300\ K}$) is characteristic for the superconducting properties of the film: the lower the resistivity, the higher the T_{zero}.

The resistivity of the $YBa_2Cu_3O_{7-\delta}$ compound

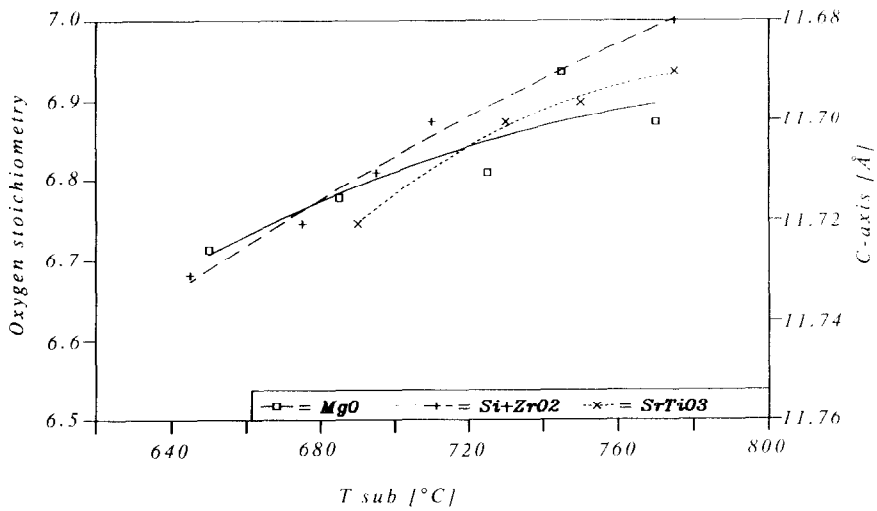

Fig. 3. The c-axis and oxygen stoichiometry of YBaCuO on three different substrates at various T_{sub} calculated from the 2θ values of the X-ray patterns, using data from ref. [10].

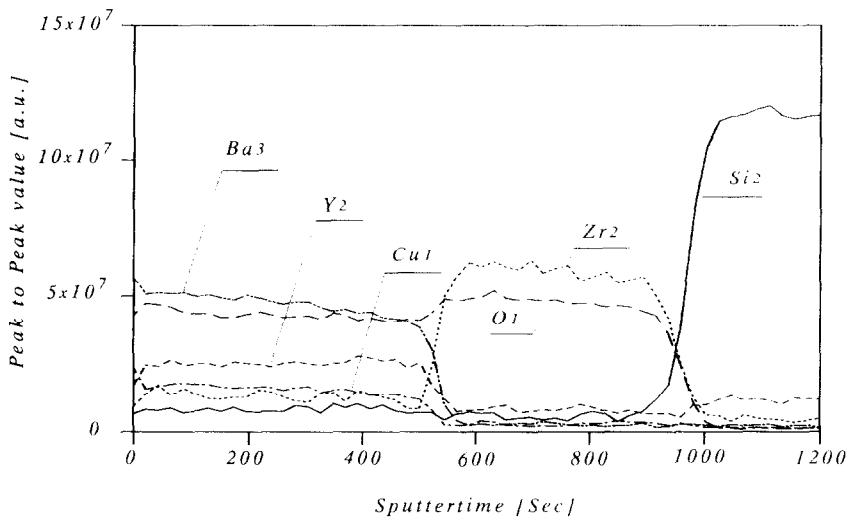

Fig. 4. Auger sputter profile of an YBaCuO film deposited on Si with a 250 nm ZrO_2 buffer layer deposited at a substrate temperature of 700°C.

shows a linear temperature behaviour between 300 and 110 K, as is well known from the literature [12]. The temperature dependent resistivity can be described by $\rho=\alpha\rho_{BG}+\rho_0+\rho_a$, with ρ_{BG} the resistivity from the classical Blach–Grüneisen theory, which for this compound leads to a linear temperature dependency in the above mentioned temperature range, using an effective transport Debye temperature of $\theta^*_D=200$ K [13]. The residual resistivity $\rho_0=\rho(T=0)$ is due to impurities and lattice imperfections and is almost temperature independent. The extra resistivity ρ_a is due to grain boundaries and additional imperfections such as interface reactions. If the grain boundaries are responsible for this extra

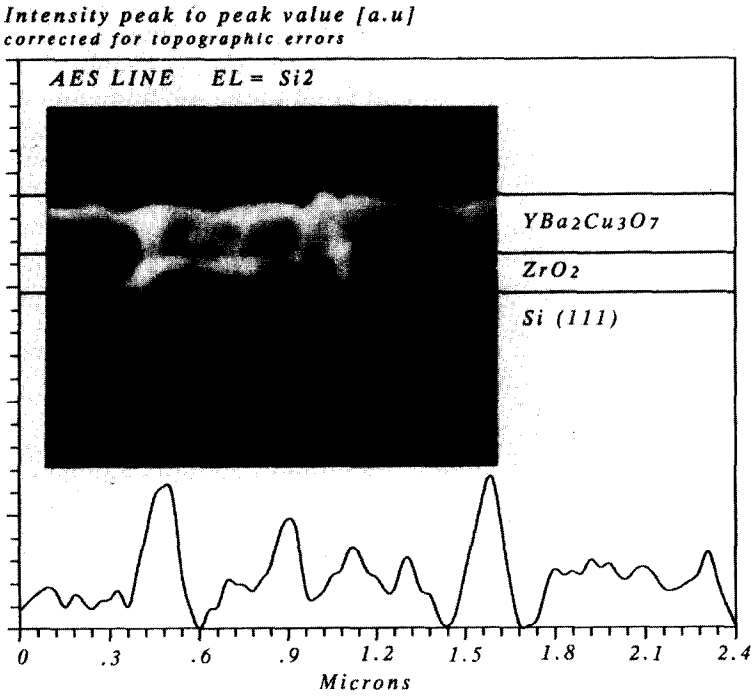

Fig. 5. SEM picture of a cleaved surface of an YBaCuO layer deposited at 750°C on Si+ZrO_2. The dots represent the intensities of the peak to peak values of Si_2 in the ZrO_2 buffer layer. The values are corrected for topographic errors.

resistivity, then their behaviour depends on the properties of the boundaries themselves. In the case of the films deposited on $SrTiO_3$ at higher substrate temperatures, ρ_a is almost negligible. We were able to fit the data of the best films to the Bloch–Grüneisen theory, using $\theta_D^* = 200$ K, and obtaining $\rho_0 = 20$ μΩcm (see fig.7). In the case of all other films, ρ_a becomes important and the determination of ρ_0 is to some extent uncertain. For this reason we used the linearly extrapolated value of the resistivity at $T = 0$ K: ρ_{EX}. The values of ρ_{EX} can be extracted directly from the measurements and appear to be a good measure of the quality of the films. From the data given in table I one can conclude that ρ_{EX} is strongly dependent on the type of substrate.

The films deposited on $SrTiO_3$ have the lowest value of ρ_{EX} ($\ll 10$ μΩcm). The ρ_{EX} of the films, deposited on MgO and Si+ZrO_2 and prepared under optimum conditions, are significantly larger, indicating the occurrence of grain boundaries. The data for J_c, $T_{ons} - T_{zero}$, and $\rho_{300\,K}$ confirms this. The critical current density in the film is limited by the grain boundaries (weak links) because of its SNS type behaviour [14]. This effect can especially be seen in the films deposited on Si+ZrO_2, where the number of grains is large due to the polycrystalline buffer layer of ZrO_2. The YBaCuO grains have the correct oxygen content, the X-ray patterns show only (00l) reflections with high intensities, and T_{ons} is almost independent of T_{sub}; in other words, the bulk properties of the YBaCuO grains are still in order and one should not expect a distribution of T_c's over the individual grains. Below the onset temperature the resistivity in the grains is zero and the grain boundaries are responsible for the resistivity. The dimensions of the grain boundaries, the measuring current and the temperature determine the transition width. We found a strong linear correlation between the transition width and the ρ_{EX} resistivity. In fig. 8 we have plotted the data for a number of films, even when they were prepared far from optimal conditions.

The substrate temperature is of great importance

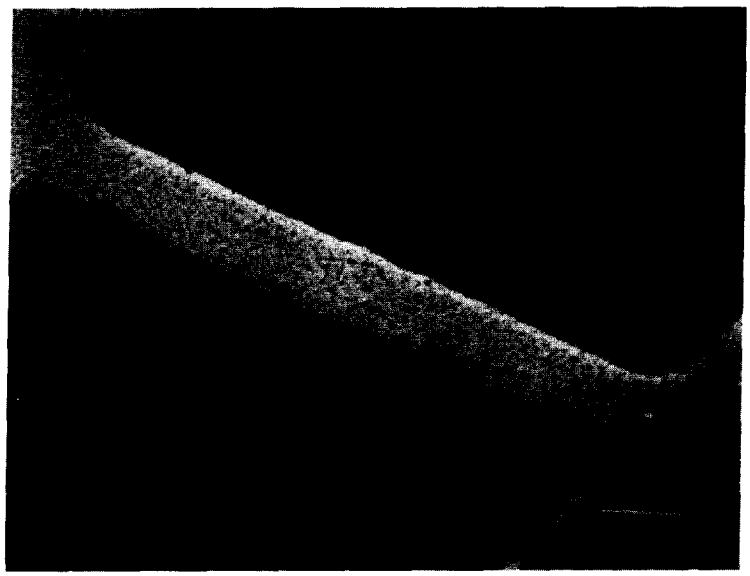

Fig. 6. SEM picture of a wet etched YBaCuO bridge on $Si+ZrO_2$ with typical dimensions of 10×100 μm^2. Notice the polycrystalline structure of the film.

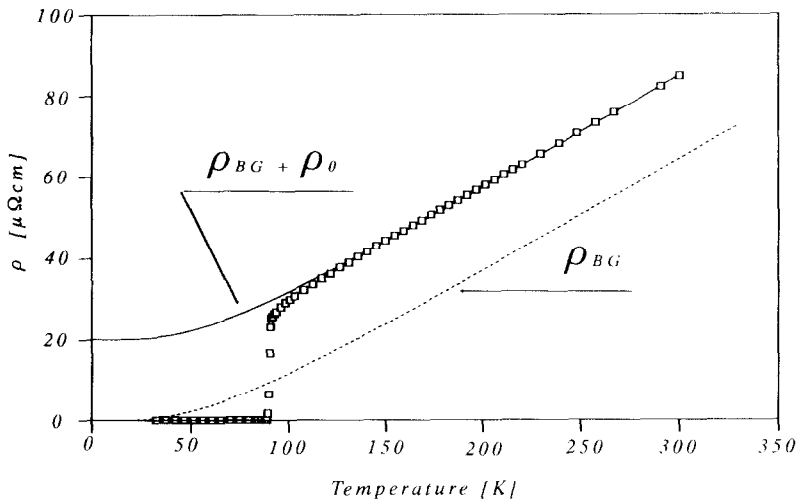

Fig. 7. Temperature dependence resistivity of an YBaCuO film on $SrTiO_3$ ablated at a substrate temperature of 775°C. The dashed line is the Bloch–Grüneisen fit with $\theta_D^* = 200$ K. The solid line is $\rho_{BG}+\rho_0$, with $\rho_0 = 20$ μΩcm.

for the fabrication of films with the correct superconducting properties. At low deposition temperatures the superconducting properties are very poor. The influence of the substrate is negligible (see fig. 1); T_{zero} values do not differ for different substrates. Although the X-ray diffraction patterns show c-axis oriented films, their intensities are 10 to 100 times smaller than the intensities of films deposited at high temperature. Below 690°C (110/103) reflections occur (see fig. 2), but their intensities are small,

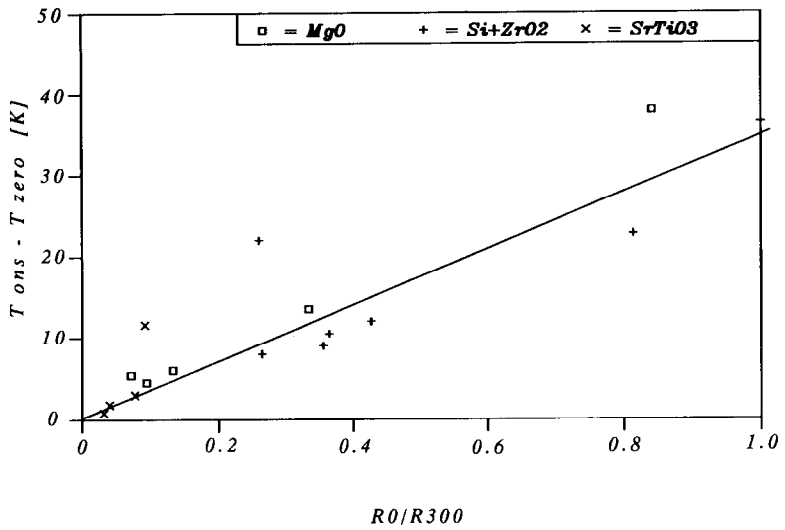

Fig. 8. Relation between the transition width and $R0/R300$ for a number of deposited YBaCuO films on different substrates.

compared to the (005) reflections. This means that the films is less crystalline and becomes amorphous. To know to what extent this effect occurs, further investigations have to be done, especially regarding the peak width of the reflections. The calculated oxygen values in the film (see fig. 3) decrease with decreasing substrate temperature. This is a bulk effect, because the influence of the oxygen content on T_{ons} behaves in the same way as indicated by Cava et al. [10].

At high substrate temperatures the influence of the substrate becomes obvious. In the case of $SrTiO_3$, the properties become better at higher substrate temperatures. The resistivity at room temperature as well as ρ_{EX} decrease. T_{zero} increases and the transition width becomes smaller (see table I). X-ray diffraction measurements only give (00l) reflections and the calculated oxygen content yields $\delta \leq 0.1$ (see fig. 5). In the case of MgO substrates the same dependence on the deposition temperature is observed, although there is an indication of an optimum temperature range from 730°C to 760°C. Nevertheless, the highest reachable T_{zero} is smaller than that for films on $SrTiO_3$. The same holds for T_{ons}. In the case of $Si+ZrO_2$ the substrate influence is remarkable. The values of $\rho_{300\,K}$ and ρ_{EX} are one order of magnitude larger than in the case of $SrTiO_3$ and MgO (see table I) and T_{zero} decreases with higher substrate temperatures (see fig. 1). X-ray diffraction measurements show only (00l) reflections and the calculated oxygen content is very high (see fig. 3). From these measurements it can be concluded that the grains have the correct stoichiometry, are fully c-axis oriented and have the correct oxygen content. It follows that the grain boundaries in the film are responsible for the broadening of the transition. The diffusion of silicon along the grain boundaries – an effect which becomes stronger at higher deposition temperatures – can be an explanation for this behaviour. The diffusion of Si along the grain boundaries is a crucial problem in the case of silicon substrates, as follows inter alia from this article. For that reason we have studied the Auger sputter profiles in more detail. These results will be published in a separate paper [11].

The X-ray diffraction patterns show some remarkable results in the case of the MgO substrates. Although the films on MgO show only (00l) reflections, their intensities are significantly smaller than those in the case of $SrTiO_3$ or $Si+ZrO_2$. An explanation could be the stress in the films on MgO. The crystal lattice of MgO (4.212 Å) deviates more from the a-axis (3.8206 Å) or b-axis (3.8852 Å) of YBaCuO than that of $SrTiO_3$ (3.905 Å), and in the case of the crystalline ZrO_2 on top of Si this stress is of less importance because of the grains and the lattice constants of ZrO_2.

Finally, we studied the influence of the laser pulse frequency. The films on $SrTiO_3$ have better properties at lower frequencies of the laser pulses, i.e. at 1 or 2 Hz compared to 10 or 15 Hz. This does not hold for films deposited on $Si+ZrO_2$. In a wide range of frequencies (1 to 20 Hz) almost no effect was found. It should be mentioned that the films on $SrTiO_3$, deposited at a pulse frequency of 15 Hz, have the same T_{zero} as in the case of $Si+ZrO_2$. From this we can conclude that films with the highest quality will be obtained with the lowest deposition rate (lowest pulse frequency of the laser), provided that the substrate is not sensitive to diffusion, as in the case of $Si+ZrO_2$.

Another fact is the difference between T_{ons} of the deposited film and T_{zero} of the target used. Although T_{zero} of the target is 93 K, it was not possible to make films with the same T_{zero} (or even T_{ons}). A possible explanation is a deficiency of copper. Energy dispersive X-ray analysis confirms this.

5. Conclusions

Laser ablation is a convenient method to produce high-quality high-T_c films on various substrates. We have shown the results on (100) $SrTiO_3$, on (100) MgO and on (111) $Si+ZrO_2$ for in situ preparation. The resistivity at room temperature and the linearly extrapolated value of the resistivity (ρ_{EX}) are a good measure of the physical properties of the film, such as the transition width and J_c. A linear correlation is found between ρ_{EX} and the transition width.

The substrate temperature is a crucial process parameter. At low deposition temperatures the films are amorphous and do not have the correct oxygen content. At higher deposition temperatures there is a distinct difference between the substrates used. Films on $SrTiO_3$ and MgO behave as high quality crystalline layers with low resistivity, high critical currents and sharp transitions. The films on $Si+ZrO_2$ show perfect c-axis orientation and high oxygen content, although the resistivity is quite high and the critical current small, indicating good bulk properties of a polycrystalline layer with weakly coupled grains. The properties of the YBaCuO layer are strongly dependent on the grain size of the buffer layer.

The 250 nm buffer layer of ZrO_2 on the Si substrate prevents diffusion of silicon into the YBaCuO layer. If one succeeds in producing a buffer layer on Si with a less granular structure, the quality of the layer is expected to be comparable with the quality of layers deposited on MgO.

Structuring by excimer laser instead of chemical etching is favoured in the case of granular films, like those on $Si+ZrO_2$.

Acknowledgements

We would like to thank A.J.H.M. Rijnders for the SEM pictures and W.A.M. Aarnink for carrying out the Auger sputter profiles and for the useful discussions concerning these measurements.

References

[1] R.B. Laibowitz, R.H. Koch, P. Chaudhari and R.J. Gambino, Phys. Rev. B35 (1987) 8821.
[2] M. Niato, R.H. Hammond, B. Oh, M.R. Beasley and T.H. Geballe, Appl. Phys. Lett. 51 (1987) 713.
[3] D. Dijkkamp, T. Venkatesan, X.D. Wu, S.A. Shaheen, N. Jisrawi, Y.H. Minlee, W.L. McLean and M. Croft, Appl. Phys. Lett. 51 (1987) 619.
[4] X.X. Xi, G. Linker, O. Meyer, E. Nold, B. Obst, F. Ratsel, R. Smithey, B. Strahlan, F. Weschenfilder and J. Geerd, J. Phys. B. Cond. Matt. 74 (1989) 13.
[5] N. Missert, R. Hammond, J.E. Mooij, V. Matijasevic, P. Rosenthal, T.H. Geballe, A. Kapitulnik, M.R. Beasley, S.S. Laderman, C. Lu, E. Garwin and R. Barton, IEEE Trans. Magn. MAG-25 (1989) 2418.
[6] B. Roas, L. Schultz and G. Endres, Appl. Phys. Lett. 53 (1988) 1557.
[7] A. Mogro-Campero, L.G. Turner and G. Kendall, Appl. Phys. Lett. 53 (1988) 2566.
[8] T. Venkasesan, E.W. Chase, X.D. Wu, A. Inam, C.C. Chang and F.K. Shokoohi, Appl. Phys. Lett. 53 (1988) 243.
[9] D.H.A. Blank, H. Kruidhof and J. Flokstra, J. Phys. D 21 (1988) 226.
[10] R.J. Cava, B. Batlogg, C.H. Chen, E.A. Rietman, S.M. Zahurak and D. Werder, Phys. Rev. B36 (1987) 2262.
[11] W.A.M. Aarnink, D.H.A. Blank, D.J. Adelerhof, J. Flokstra, H. Rogalla, A. van Silfhout, R. de Reus and F.W. Saris, to be published.
[12] A. Kapitulnik, Physica C 153–155 (1988) 520.
[13] S. Martin, M. Gurvitch, C.E. Rice, A.F. Hebard, P.L. Gammel, R.M. Flemming and A.T. Fiory, Phys. Rev. B39 (1989) 9611.
[14] B. Haüser, B.B.G. Klopman, G.J. Gerritsma, J. Gao and H. Rogalla, Appl. Phys. Lett. 54 (1989) 1368.